Acta Cryst. (1994). B**50**, 589–596

Crystallography of Metal Picrates. II.* Crystal Structure of Yellow Thallium(I) Picrate; Relations Among Various Metal(I) Picrate Phases

BY MARK BOTOSHANSKY, FRANK H. HERBSTEIN AND MOSHE KAPON

Department of Chemistry, Technion-Israel Institute of Technology, Haifa 32000, Israel

(*Received* 7 *October* 1993; *accepted* 8 *February* 1994)

Abstract

Thallium(I) picrate, $Tl^+.C_6H_2N_3O_7^-$ is an organic salt which has been known for 125 years to exist in two crystalline phases; one phase (orange–red prisms) was reported, from solubility measurements, to be stable below 319 K and the other (yellow needles) above this temperature [Rabe (1901). *Z. Phys. Chem.* **38**, 175–184]. The transition temperature was confirmed by dilatometry [Cohen & Moesveld (1920). *Z. Phys. Chem.* **94**, 450–464]. The crystal structure of the red prisms has been reported [Herbstein, Kapon & Wielinski (1977). *Acta Cryst.* B**33**, 649–654] and that of the yellow needles is reported here. In both phases there are stacks of anions with interposed cations, but the detailed arrangements are different (for example, the shortest $Tl^+\cdots O$ distance is 0.2 Å less in the yellow polymorph than in the red). The transition between the two phases is a single crystal of red to polycrystalline yellow, showing some preferred orientation. Differential scanning calorimetry (DSC) and X-ray powder diffraction show that the red phase is converted into the yellow at 423 K in the absence of solvent. DSC measurements give the enthalpy change of this endothermic conversion as 5.0 kJ mol^{-1}. The high-temperature yellow phase decomposes before melting. Yellow crystals cooled slowly from above 423 K do not revert to the red form. In the presence of a small amount of solvent (water), conversion of the red into the yellow phase is visible at 333 K. Our explanation is that the thermodynamic equilibrium temperature is indeed 319 K, that the forward transformation (red to yellow) in the dry state has such a large activation energy that it is fast enough for measurement by dynamic DSC only in the 423 K region, but that the rate is appreciably increased by the presence of solvent. The reverse transformation (yellow to red) occurs only below 319 K, where it is very slow in the dry state but takes a few days in the presence of solvent. The details of the structure determination (at 298 K) are: yellow laths (stable above 319 K): M_r = 432.47, λ(Mo $K\alpha$) = 0.71069 Å, $F(000)$ = 784, monoclinic, μ(Mo $K\alpha$) = 16.9 mm^{-1}, $P2_1/a$, a = 15.431 (5), b = 15.830 (5), c = 3.951 (2) Å, β = 91.06 (10)°, V = 965.0 $Å^3$, Z = 4, D_m = 2.993 [290 K, Rabe (1901)], D_x = 2.978 g cm^{-3}, R_{int} = 0.0268, $R(F)$ = 0.0394, wR = 0.0388 [based on 1701 independent reflections with $F>3\sigma(F)$]. Cell dimensions have been measured for the red and yellow phases over the temperature ranges 290–370 and 290–490 K, respectively.

1. Introduction

In the first report (1866) of its occurrence, thallium(I) picrate was described by Kuhlmann and, separately, by Böttger as an explosive material, crystallizing as yellow needles or plates. Two years later, Cloiseaux & Lamy reported that there was a second, red form. A more extended investigation was carried out by Rabe (1901), who gave references to the earlier work. Rabe showed that when TlOH and picric acid are dissolved in water or alcohol at about neutral pH, yellow needles of thallium(I) picrate crystallize first; according to Cohen & Moesveld (1920), this always occurs, irrespective of crystallization temperature. The yellow needles change over a few days to red prisms if left in contact with solvent at room temperature. Both needles and prisms are indefinitely stable at room temperature under dry conditions. Rabe (1901) investigated the relative stabilities of the two phases by measuring their solubilities in water and methanol as a function of temperature and found the equilibrium temperature of red⇔yellow forms to be 319 K, with red stable below this temperature. He also reported that red crystals heated at 349 K for 24 h showed an appreciable amount of yellow spots and that there was instantaneous transformation of red to yellow at 403 K and above; the reverse transformation occurred below 313 K but was very sluggish. The transformations were found to be remarkably accelerated by the presence of small amounts of solvent. Rabe's conclusion was: 'Das Thallopikrat tritt in zwei physikalisch isomeren Formen auf, deren Umwandlungspunkt bei 46°C liegt'. Cohen & Moesveld (1920; see also Cohen, 1929) repeated some of Rabe's work, confirmed the transition point as 319 K from dilatometric measurements (they used 150 g of each of the red and yellow polymorphs and moistened their samples to accelerate the transformation) and found ΔV to be *ca* 6%. They reported that the red to yellow transformation occurred in dry samples at 349 and 403 K, but not at 373 K.

* Part I: Herbstein, Kapon & Wielinski (1977).

The crystallography of the polymorphs was first studied by Stevanovic (1903), who reported the red polymorph to be monoclinic and the yellow triclinic (pseudo-monoclinic). We have determined unit cells for some Group IA picrates and compared our results with those of Stevanovic (1903) and others; we have also reported the crystal structure of red thallium(I) picrate, which is monoclinic (Herbstein, Kapon & Wielinski, 1977; HKW77). Although our results for this phase are not very precise by more modern standards, we have decided not to repeat this work as an accurate structure determination has since been reported for the isomorphous caesium picrate by Schouten, Kanters & Poonia (1990; SKP90), while Dr H. H. Cady has determined the structure of the isomorphous rubidium picrate (unpublished). We now report the structure of yellow thallium(I) picrate, which is actually monoclinic, and a study of the relationship and transformations between the red and yellow phases.

Rubidium, caesium and red thallium picrates are isomorphous (similar cell dimensions, same space group, similar structures). We have confirmed earlier results of Stammler (1968) regarding the atmospheric pressure–variable-temperature phase relations for the M^1 picrates, where M^1 = NH_4, Rb, Cs. We repeat here a summary of crystal data for M^1 picrates, as our earlier survey contained a number of errors, kindly pointed out to us by Dr Cady in 1977 (private communication).

Thallium (and other) picrates must be handled with care both because of the toxicity of thallium salts and the sensitivity of the picrates to explosion (Sax, 1979). However, we have not experienced difficulties with the small quantities required for the present studies.

2. Determination of the crystal structure of yellow thallium(I) picrate

2.1. *Experimental*

Thallium(I) picrate was prepared by the reaction of equimolar amounts of TlOH and picric acid in distilled water. Long yellow laths, elongated along [001], were obtained by slow cooling from 313 K [we have noticed (an experiment by Noga Gasper) that the red polymorph is obtained directly if small amounts of thiourea are present in the solution, but we have not attempted to follow up this observation]. After preliminary diffraction photography (Ni-filtered Cu $K\alpha$), cell dimensions and the space group were determined on a Philips PW 1100 four-circle diffractometer (graphite-monochromated Mo $K\alpha$; λ = 0.71069 Å) using a crystal of triangular cross-section with edges of 0.15 and 0.29 mm in length, set with [001] approximately along φ; the (110), (010) and (001) faces were developed. 24 reflections with $6 \le 2\theta \le 13°$ were used for the cell dimension determination; our results agree well with those of HKW77. In all, 2728 reflection intensities were measured by the $\omega/2\theta$ scan method, indices lying within the limits $-18 \le h \le 18$, $0 \le k \le 18$, $0 \le l \le 4$, with $(\sin\theta/\lambda)_{max}$ = 0.595 Å^{-1}. Absorption corrections were calculated for the measured crystal shape; transmission factors ranged from 0.26 to 0.12. Intensities of three standard reflections (021, $1\bar{4}1$, 600) were measured at intervals of 120 min; the crystal and measuring system were stable to within 2% over the 48 h measuring period, without any decay being evident. R_{int} (= 0.0268) was calculated from a comparison of symmetry-equivalent reflections. After culling redundant reflections, 1701 unique reflections with $F_{obs} \ge 3\sigma(F_{obs})$ remained. The structure was solved by the Patterson method and refined using *SHELX*76 (Sheldrick, 1976); 162 variables were refined, with anisotropic displacement factors for non-H atoms and isotropic displacement factors for H atoms. Neutral atom scattering factors (Cromer & Waber, 1974) with dispersion corrections (Cromer, 1974) were used.

Table 1. *Fractional atomic coordinates and equivalent isotropic displacement parameters* (Å^2)

$U_{eq} = (1/3)\Sigma_i\Sigma_j U_{ij} a_i^* a_j^* \mathbf{a}_i.\mathbf{a}_j$.

	x	y	z	U_{eq}
Tl	0.31677 (2)	0.45874 (2)	0.43422 (10)	0.0472 (1)
C(1)	0.4293 (5)	0.2995 (6)	0.9013 (20)	0.038 (2)
C(2)	0.4055 (5)	0.2177 (6)	0.7662 (24)	0.041 (2)
C(3)	0.4605 (6)	0.1496 (6)	0.7525 (26)	0.045 (2)
C(4)	0.5444 (5)	0.1589 (6)	0.8631 (23)	0.040 (2)
C(5)	0.5768 (5)	0.2337 (6)	0.9899 (25)	0.045 (2)
C(6)	0.5190 (5)	0.3006 (5)	1.0108 (10)	0.036 (2)
N(1)	0.3168 (4)	0.2056 (5)	0.6326 (23)	0.047 (2)
O(1)	0.2786 (5)	0.2636 (5)	0.5013 (26)	0.079 (2)
O(2)	0.2862 (5)	0.1358 (6)	0.6521 (35)	0.108 (4)
N(2)	0.6040 (5)	0.0869 (6)	0.8487 (25)	0.060 (2)
O(3)	0.5786 (7)	0.0207 (6)	0.7210 (38)	0.126 (4)
O(4)	0.6764 (4)	0.0939 (6)	0.9596 (26)	0.080 (2)
N(3)	0.5554 (5)	0.3805 (5)	1.1435 (20)	0.046 (2)
O(5)	0.6295 (5)	0.3996 (5)	1.0642 (24)	0.069 (2)
O(6)	0.5117 (5)	0.4240 (5)	1.3324 (24)	0.076 (2)
O(7)	0.3799 (4)	0.3623 (4)	0.9229 (17)	0.049 (2)

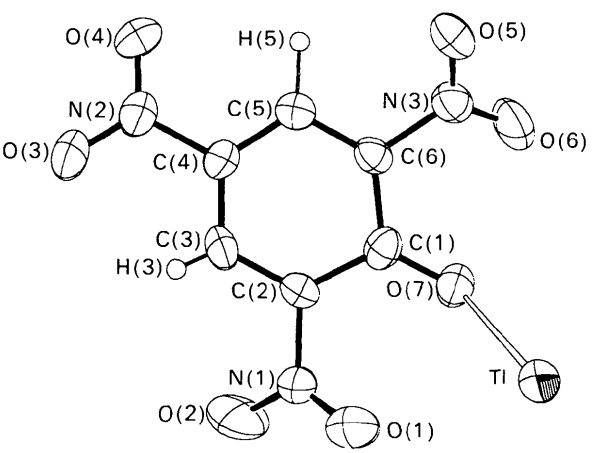

Fig. 1. *ORTEP* (Johnson, 1965) diagram showing the numbering scheme and thermal ellipsoids drawn at 50% probability levels for the atoms of the asymmetric unit.

The final weighting scheme was $w = 0.860/[\mathrm{var}(F_{meas}) + 0.00160(F_{meas})^2]$. The final R_F value was 0.0392 (R_W = 0.0398). The largest value of $|\Delta/\sigma|$ in the final refinement cycle was 0.5 (average value 0.1) and $\Delta\rho_{max}$ and $\Delta\rho_{min}$ in the final difference map were 1.3 and 1.8 e Å^{-3} respectively, both peaks being within 0.5 e Å^{-3} of thallium. Atomic parameters are given in Table 1* and the numbering scheme in Fig. 1; values of U_{eq} were calculated following Fischer & Tillmanns (1988), and their e.s.d.'s following the orthic and isotropic approximation of Schomaker & Marsh (1983). The U_{ij} values (deposited) are unexceptional apart from the large U_{33} values of the nitro O atoms: O(1), 0.108(11); O(2), 0.190(12); O(3), 0.207(14); O(4), 0.124(7); O(5), 0.105(7); O(6), 0.108(7) (Å^2).

3. Structure of the picrate ion; the immediate environment of Tl^+

The dimensions of the picrate ion (Table 2) are compatible with other, more precise, published values [for a recent summary, see Botoshansky, Herbstein & Kapon (1994)]. The large values of U_{33} for the O atoms of the nitro groups are evidence of appreciable libration of the ion as a whole and of torsional motion of the nitro groups about the C—N bonds. We have not considered analysis of the thermal motion to be justified, in view of the large absorption corrections.

Each Tl^+ is surrounded by nine O atoms (Fig. 2), with distances ranging from 2.63 to 3.24 Å, the closest neighbours being two phenoxide oxygens at 2.63 and 2.72 Å, separated by translation along [001]. The immediate environment of the Tl^+ ion is not very different from that found in the red phase – there is a trigonal prism of oxygens around the cation and each of the rectangular faces is capped with an oxygen (*cf.* Fig. 2 of HKW77 and Fig. 2 of SKP90). Thus, we infer, as we did previously for the red polymorph, that the $6s^2$ lone pair of the Tl^+ ion is not stereochemically active. Analysis of the closest metal-to-oxygen distances in the three metal(I) picrates for which structures are known (M^I = K^+, Cs^+, red Tl^+) shows that if the oxygen radius is taken as 1.26 Å, then the derived ionic radii of the cations agree well with the effective ionic radii given by Shannon (1976) for eight coordination. Our conclusion is that these three crystals can be classified as ionic. However, the shortest $Tl^+\cdots O$ distance in yellow thallium picrate is 0.2 Å shorter than that in the red polymorph (where there are nine short $Tl^+\cdots O$ distances in the range 2.83–3.22 Å, the closest distance being to phenoxide oxygen); this suggests an appreciable covalent contribution, especially as there is little change in the form of the coordination polyhedron.

The Tl^+ environment is unsymmetrical in two polymorphic thallium salts of the antibiotic lasalocid A (Aoki, Suh, Nagashima, Uzawa & Yamazaki, 1992) and in other structures quoted by these authors. As the shortest $Tl^+\cdots O$ distances in the lasalocid A polymorphs are 2.68 (1) and 2.62 (1) Å, respectively, we infer that some covalent bonding also occurs in these structures. Some other examples were noted in HKW77.

Table 2. *Selected geometric parameters* (Å, °)

Tl—O(7)	2.633 (6)	C(5)—C(6)	1.39 (1)
C(1)—C(2)	1.45 (1)	C(6)—N(3)	1.48 (1)
C(1)—C(6)	1.44 (1)	O(1)—N(1)	1.20 (1)
C(1)—O(7)	1.26 (1)	O(2)—N(1)	1.21 (1)
C(2)—C(3)	1.37 (1)	O(3)—N(2)	1.22 (1)
C(2)—N(1)	1.47 (1)	O(4)—N(2)	1.20 (1)
C(3)—C(4)	1.37 (1)	O(5)—N(3)	1.23 (1)
C(4)—C(5)	1.38 (1)	O(6)—N(3)	1.23 (1)
C(4)—N(2)	1.47 (1)		
O(1)—Tl—O(7)	55.8 (2)	C(1)—C(6)—C(5)	126.0 (7)
C(2)—C(1)—C(6)	110.9 (7)	C(1)—C(6)—N(3)	118.2 (6)
C(2)—C(1)—O(7)	125.7 (7)	C(5)—C(6)—N(3)	115.7 (6)
C(6)—C(1)—O(7)	123.4 (7)	C(2)—N(1)—O(1)	120.0 (7)
C(1)—C(2)—C(3)	124.4 (7)	C(2)—N(1)—O(2)	117.4 (8)
C(1)—C(2)—N(1)	118.5 (7)	O(1)—N(1)—O(2)	122.5 (8)
C(3)—C(2)—N(1)	117.1 (7)	C(4)—N(2)—O(3)	119.0 (8)
C(2)—C(3)—C(4)	119.0 (8)	C(4)—N(2)—O(4)	119.7 (8)
C(3)—C(4)—C(5)	123.1 (8)	O(3)—N(2)—O(4)	121.3 (9)
C(3)—C(4)—N(2)	119.6 (8)	C(6)—N(3)—O(5)	118.0 (7)
C(5)—C(4)—N(2)	117.3 (7)	C(6)—N(3)—O(6)	119.1 (7)
C(4)—C(5)—C(6)	116.6 (7)	O(5)—N(3)—O(6)	122.9 (8)

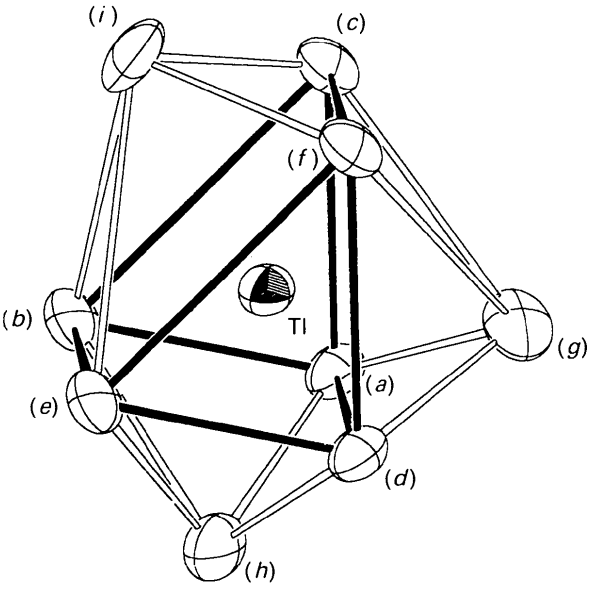

Fig. 2. Environment of the Tl^+ ion in yellow thallium picrate. The trigonal prism of oxygens about Tl^+ is emphasized, the capping oxygens being joined to the vertices by lighter lines. The oxygens are identified by *ORTEP* reference codes with the symmetry operations numbered as follows: (i) x, y, z; (ii) $\frac{1}{2} - x, \frac{1}{2} + y, -z$; (iii) $-x, -y, -z$; (iv) $\frac{1}{2} + x, \frac{1}{2} - y, z$. The $Tl\cdots O$ distances (Å) [$\sigma(Tl\cdots O) \simeq 0.007$ Å] are as follows: (*a*) [O(7) 55401] 2.726; (*b*) [O(4) 45404] 2.959; (*c*) [O(5) 66603] 3.107; (*d*) [O(7) 55501] 2.633; (*e*) [O(4) 45504] 3.140; (*f*) [O(5) 66703] 3.096; (*g*) [O(6) 55401] 3.092; (*h*) [O(1) 55501] 3.156; (*i*) [O(2) 55602] 3.236.

* Lists of structure factors, anisotropic displacement parameters and variations of cell parameters with temperature and a solubility diagram have been deposited with the IUCr (Reference: MU0313). Copies may be obtained through the Managing Editor, International Union of Crystallography, 5 Abbey Square, Chester CH1 2HU, England.

4. Description of the crystal structure

The crystal structure, which is different from those of the isomorphous pair of NH_4 and K picrates, and, in some respects, from those of the differently isomorphous triplet of Rb, Cs and (red) Tl^I picrates, is based on columns of translationally equivalent Tl^+ ions arranged along [001], each such column being surrounded by four stacks of translationally equivalent picrate ions [as shown in the *ORTEP* (Johnson, 1965) stereodiagram in Fig. 3]. Red thallium picrate is shown in Fig. 4; the picrate ions have been oriented in matching fashion in order to facilitate comparison between the structures. These figures are deceptively similar in that both have columns of picrate ions separated by columns of Tl^+ ions; in projection there are analogous sheets in the (100) planes of both cells. However, the details of arrangement within and between sheets are different. In yellow thallium picrate, adjacent columns within a sheet are related by centres of symmetry, and adjacent sheets by *a* glide planes (normal to [010]). In red thallium picrate, adjacent columns within a sheet are related by twofold screw axes (parallel to [010]), and adjacent sheets by centres of symmetry.

In formal terms, transformation of red into yellow thallium picrate requires alteration of the detailed packing arrangements of the Tl^+ and picrate ions, as discussed above. Spatial considerations rule out a direct interconversion, so the transformation is expected to proceed by a nucleation and growth mechanism, and indeed diffraction photography shows that the transformation is from a single crystal of the red phase to a pseudomorph of the polycrystalline yellow phase.

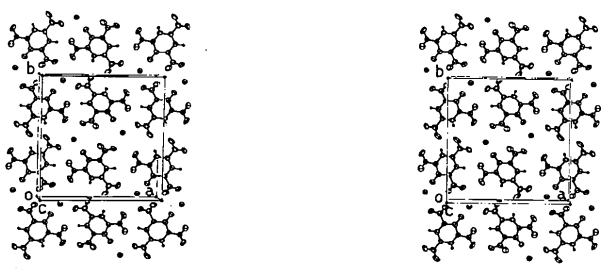

Fig. 3. *ORTEP* (Johnson, 1965) stereodiagram of the crystal structure of yellow thallium picrate. The ellipsoids are drawn at 50% probability levels.

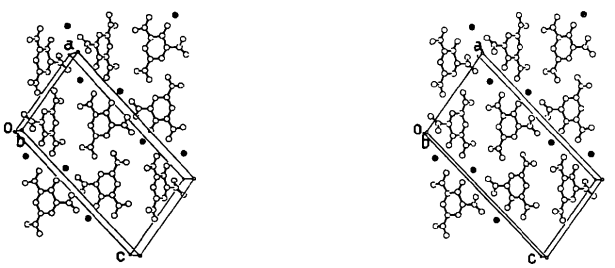

Fig. 4. *ORTEP* (Johnson, 1965) stereodiagram of the crystal structure of red thallium picrate. The ellipsoids are drawn at 50% probability levels.

5. Experimental study of the transformation between the two phases

5.1. *DSC measurements*

Dynamic DSC curves were determined for *dry*, *powdered* samples of red and yellow phases using a Mettler TA3000 DSC apparatus. The heating curve of the red phase showed a reasonably sharp endotherm peaking at 423 K, the enthalpy of conversion of red to yellow being 5.0 kJ mol^{-1}. The cooling curve was featureless, as were the heating and cooling curves for the yellow phase. When the sample consisted of a number of single crystals of the red phase, the endotherm extended over the region 383–423 K (Fig. 5). Stammler (1968) reported that 'the [DTA (differential thermal analysis)] thermogram of the orange (our red) modification shows a broad endotherm at 423 K, which is associated with a colour change to yellow.' The nature of Stammler's samples (single crystals or powder) was not specified.

We also measured isothermal DSC curves at 333, 343 and 353 K for *ca* 5 mg samples of powdered red thallium picrate, moistened with a drop of water,* with the reference pan containing a similar amount of water and both pans being sealed. Complete conversion to yellow occurred after 33 min at 343 K and 14 min at 353 K. Conversion started after 60 min at 333 K and continued, in an irregular fashion, for another *ca* 60 min. We were not able to make quantitative measurements on the DSC output because of uneven background. However, these results are puzzling in that the thermal effects are exothermic and not endothermic, as expected.

* We are grateful to Professor Mark Ratner (Northwestern Univ.) for suggesting this stratagem.

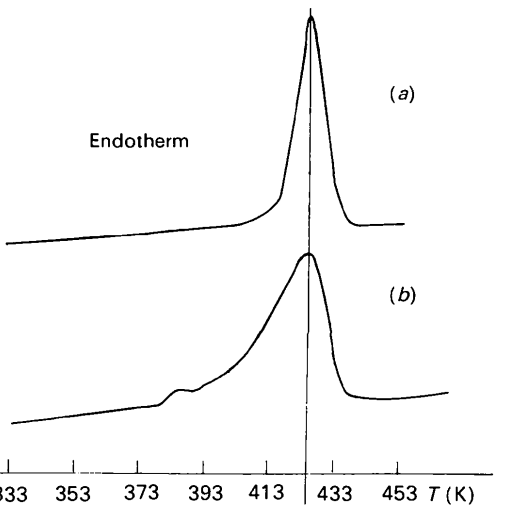

Fig. 5. DSC traces for (*a*) multi-single crystal and (*b*) powdered samples of red thallium picrate. Heat changes are measured along the ordinate, with absorption upwards; the peaks thus represent endotherms. The curves are on approximately the same scale; sample weights were *ca* 5 mg.

Perhaps the water plays an unexpected role. Clearly further investigation is needed.

5.2. *Dependence of cell dimensions on temperature*

Single crystals of the red and yellow phases were sealed into capillaries and mounted on a Nonius crystal heating device (design of Tuinstra & Fraase Storm, 1978), modified for attachment to the Philips four-circle diffractometer. The temperature scale was calibrated by reference to the (known) melting points of a number of compounds. Cell dimensions were measured using Mo $K\alpha$. The temperature range for the red phase was 293–373 K; splitting of reflections above 373 K showed that the crystal was beginning to incur damage of an unspecified nature. Similar measurements were made for the yellow phase, up to a maximum of 483 K; the yellow crystals remained intact over the whole temperature range. The values of a, b, c, β and V for both phases are given in Table E (deposited), and the corresponding diagrams in Figs. 6, 7 and 8. ΔV (red to yellow) is 14.6 Å^3/formula unit at 293 K and 13.9 Å^3/formula unit at 363 K, or about 6%. Our value for ΔV agrees well with that given by Cohen & Moesveld (1920, pp. 458–459) from dilatometry.

The thermal expansion tensors above and below T_c have been determined (Table 3) from the thermally induced changes of the Bragg angles of certain reflections using a *FORTRAN* program (*ALPHA*) written by Jessen & Küppers (1989, 1991), which also diagonalizes the tensor. We have used the temperature pairs 293, 363 K (red) and 293, 423 K (yellow) for these calculations.

For the red phase all three principal components of the symmetrical second-order tensor $[\alpha_{ij}]$ are positive. Thus, the representation quadric is a triaxial ellipsoid. For the yellow phase, two of the principal components are positive and one is negative. Thus, the representation quadric is an hyperboloid of one sheet (Nye, 1967,

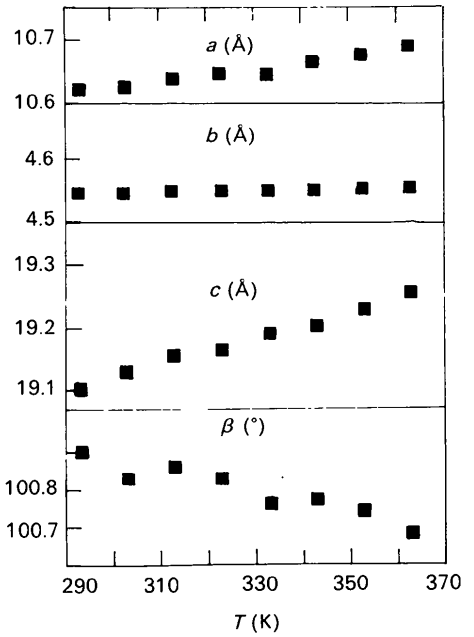

Fig. 6. Variation of a, b, c (Å) and β (°) as a function of temperature for red thallium picrate.

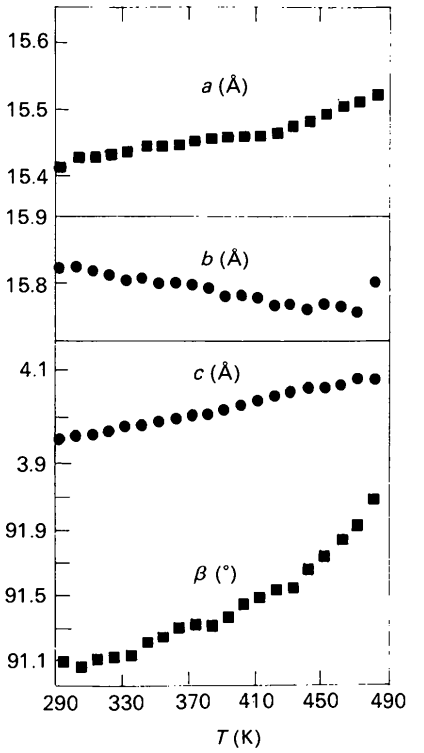

Fig. 7. Variation of a, b, c (Å) and β (°) as a function of temperature for yellow thallium picrate.

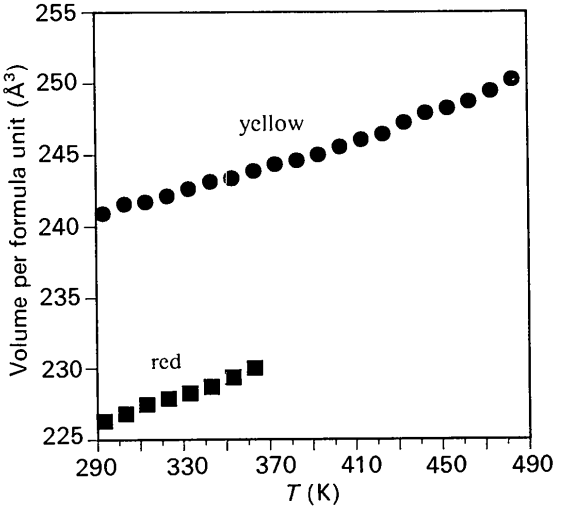

Fig. 8. Volume (Å^3) per formula unit for the two phases as a function of temperature.

Table 3. *Coefficients* α_{ij} $(10^{-6}\,K^{-1})$ *of the thermal expansion tensor for the red and yellow polymorphs of thallium picrate*

Temperature interval	α_{11}	α_{22}	α_{33}	α_{13}
293–363 K red phase	106 (12)	21 (10)	95 (17)	48 (21)
293–423 K yellow phase	26 (8)	−27 (7)	168 (8)	−40 (15)

The principal components, α_i, and the angles between the α_i and the orthonormal crystal axes $\mathbf{d}_{100}$, **b** and **c** are as shown below.

ΔT and phase	Eigenvalues $(10^{-6}\,K^{-1})$	Eigenvector angles		
293–363 K	21 (10)	90	180	90
red phase	52 (23)	132 (3)	90	42 (3)
	149 (23)	42 (3)	90	48 (3)
293–423 K	−27 (7)	90	0	90
yellow phase	16 (10)	15 (0.3)	90	75 (5)
	178 (9)	105 (5)	90	15 (0.3)

p. 18). The representation quadric of the yellow phase is shown in Fig. 9.

5.3. *Determination of the equilibrium transformation temperature*

The thermodynamic equilibrium temperature between the red and yellow phases was determined by Rabe (1901) from measurements of the solubilities of the two phases in water and methanol. The analytical method involved equilibrating red (or yellow) crystals with solvent at particular temperatures and then determining the amount of dissolved material by heating known quantities of solution to dryness. We reproduce an excerpt from Rabe's values in Fig. 10, covering the temperature range 307–332 K (a full diagram for the range 273–343 K has been deposited). The only other relevant value that we have found is due to Osake (1949, seen in the abstract only), who measured the solubility of thallium picrate (polymorph not specified) in aqueous salt solutions at 298 K; a solubility of 11.12 mmol l^{-1} of water at zero added salt is given in the abstract, in good agreement with Rabe's value of 10.99 mmol per 1000 g of water for the red polymorph.

The differences between the solubilities of the polymorphs are small and thus it is fortunate that confirmation of the 319 K value has been obtained from the dilatometric measurements of Cohen & Moesveld (1920), although details were not given. Cohen (1929, p. 166) states that 'according to recent measurements (nature not specified but presumably dilatometry)...in my laboratory, the transformation point is 317 K...'.

6. Discussion of the transformation between the two phases

The experimental results for thallium(I) picrate can be explained as follows. The true thermodynamic equilibrium temperature between red and yellow phases is 319 K, as found by Rabe (1901) from solubility measurements and Cohen (1929) from dilatometry. The yellow phase crystallizes first at room temperature in a metastable condition and then dissolves and recrystallizes as the stable red phase. This is an illustration of Ostwald's law of successive reactions, which we quote in Mellor's version [1956; see also Findlay (1951), pp. 46–60] – "if a chemical process takes place with the formation of a series of intermediate compounds,

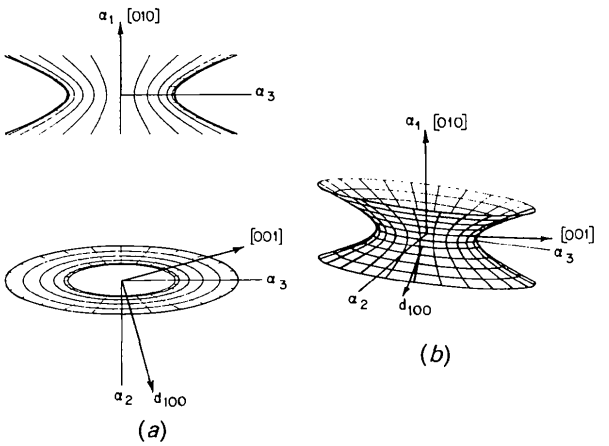

Fig. 9. Diagrams of the representation quadric (hyperboloid of one sheet) of the thermal expansion tensor of the yellow phase of Tl picrate. Three views of the quadric are shown: (*a*) down two of the principal axes and (*b*) a bimetric view. The principal axes, α_i, of the quadric are shown and the directions of the orthogonal crystal axes, $\mathbf{d}_{100}$, **b** and **c**, have been inserted in the diagram. The imaginary axis of the tensor (α_1) is parallel to **b**; $\mathbf{d}_{100}$ and **c** lie in the α_2, α_3 plane. Diagrams by Dr A. Banai.

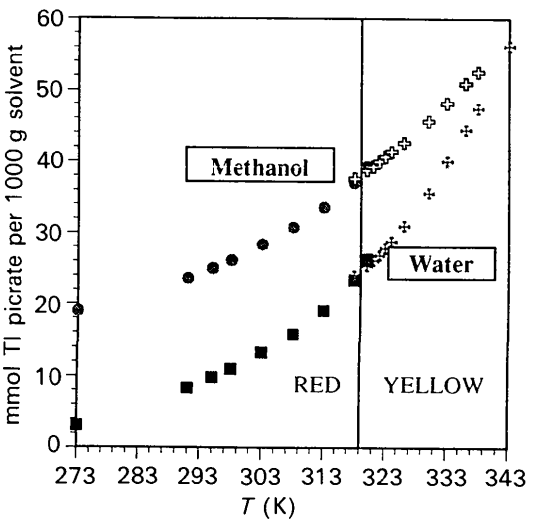

Fig. 10. Detail of the solubilities of the red and yellow phases of thallium picrate in water and methanol in the temperature range 307–332 K [taken from Rabe (1901)]. The vertical line separates the regions of phase stability as inferred from this diagram. The curves are guides to the eye.

Table 4. *Crystal data* (298 K, 1 atm) *for metal*(I) *picrates*

Compound	a (Å)	b (Å)	c (Å)	β (°)	Space group	Z	Volume per formula unit (Å^3)	Ref.
Group I								
NH_4 picrate	13.45 (4)	19.74 (5)	7.12 (2)	—	*Ibca*	8	236.3	(*a*)
K picrate	13.33	19.09	7.14	—	*Ibca*	8	227.1	(*a*)
	13.333 (4)	19.112 (4)	7.118 (5)	—	*Ibca*	8	226.73	(*b*)
Group II								
Rb picrate	10.594 (12)	4.564 (4)	19.161 (22)	101.38 (9)	$P2_1/c$	4	227.1	(*c*)
Cs picrate	10.721	4.676	19.211	101.33	$P2_1/c$	4	236.1	(*c*)
	10.811 (1)	4.701 (4)	19.404 (1)	101.41 (1)	$P2_1/c$	4	241.67 (3)	(*d*)
Tl(I) picrate (red)	10.610 (1)	4.548 (5)	19.148 (2)	101.1 (1)	$P2_1/c$	4	226.76	(*e*)
Group III								
Tl(I) picrate (yellow)	15.431 (5)	15.830 (5)	3.951 (5)	91.06 (10)	$P2_1/a$	4	241.24	(*f*)

(*a*) Maartman-Moe (1969); (*b*) Palenik (1972); (*c*) Cady (1977), private communication; (*d*) Schouten, Kanters & Poonia (1990); (*e*) Herbstein, Kapon & Wielinski (1977); (*f*) Present paper.

that compound which involves the smallest expenditure of available energy will be formed first, and so on. According to H. W. B. Roozeboom, observations show merely that [this] 'law' is sometimes applicable." There is a large barrier to the transformation from red to yellow, which thus occurs at an appreciable rate only above 373 K, as shown by our DSC results and the earlier results of Rabe (1901) and Cohen (1929). When the yellow phase obtained above 423 K is cooled, it becomes thermodynamically unstable only below 319 K, where the rate of the reverse transformation from yellow to red is very slow in the solid state. The reason for the large activation energy is not clear; the two phases have structures of the same type (salt of metal cation and organic anion) and the arrangements of the ions are rather similar. Qualitatively, we would not have expected the activation energy for the transformation to be large.

The behaviour of thallium picrate is not unique. Taguchi, Hirota, Maeda, Yasui & Iwasaki (1993) report that *N*-picryl-*p*-toluidine crystallizes in two polymorphs, orange transforming into red just below the melting point. Both polymorphs crystallize in different orientations of space group $P2_1/a$, as found for thallium picrate. The thermodynamic equilibrium temperature was not reported. Chattaway & Wünsch (1916) found, using the solubility method described above, that the enantiotropic transition point between pale yellow monoclinic phthalylphenylhydrazide (now called *N*-anilinophthalimide) and the deep yellow orthorhombic polymorph is at 282.4 K, and that between pale yellow monoclinic phthalylphenylmethylhydrazide [now called *N*-(*N*-methylanilino)phthalimide] and the orange triclinic polymorph is at 328.25 K. These values were determined by noting when the phases appeared and disappeared on crystallization from solutions held at different temperatures. It was noted that, on cooling an alcoholic solution of *N*-(*N*-methylanilino)phthalimide, orange crystals were obtained first; if this modification is allowed to remain suspended in alcohol for some days, pale yellow crystals of the monoclinic modification make their appearance and grow at the expense of the orange crystals, which become etched, dissolve away and finally disappear. Here also the solubility curves merge into one another (*cf.* Fig. 10) rather than cross abruptly. The crystallography of the two pairs of polymorphs was established by T. V. Barker using goniometric methods and we are now determining the crystal structures.

The hydrogen-bonded molecular compound *N*-methylurea–oxalic acid (2:1) is a system with both similar and different features (Harkema, Brake & Meutstege, 1979). There is an orthorhombic polymorph stable below 182 K and a monoclinic polymorph stable above 182 K [at 182 K, an exothermic and irreversible phase transition takes place, the monoclinic changing (on cooling) into the orthorhombic modification]. Cell dimensions were measured for the orthorhombic polymorph over the temperature range 120–295 K and for the monoclinic polymorph over the range 205–295 K. Thus, the orthorhombic polymorph, stable below 182 K, can be superheated to 295 K (at least), in analogy to red thallium picrate. However, the monoclinic polymorph cannot be supercooled below the thermodynamic transition temperature in contrast to the behaviour of yellow thallium picrate (it is our high-temperature phase which shows irreversible behaviour, but their low-temperature phase). The orthorhombic polymorph was prepared at 295 K by fast evaporation of an aqueous solution of the components in a stoichiometric ratio and the monoclinic polymorph by slow evaporation. Thus, at room temperature, the

metastable orthorhombic polymorph crystallizes first and then the stable monoclinic polymorph; it was not stated whether an orthorhombic to monoclinic conversion (either in the solid or *via* dissolution) occurred at 295 K. The structures of the two phases were determined at 295 K and are based on different arrangements of (essentially) the same type of layer.

The pyridinium picrate system is probably another example (Botoshansky, Herbstein & Kapon, 1994).

7. General survey of the anhydrous metal(I) picrates

7.1. *Crystallography*

The anhydrous metal(I) picrates fall into three structurally isomorphous groups: (i) NH_4 and K picrates; (ii) Rb, Cs and red Tl^I picrates; (iii) yellow Tl^I picrate. The room-temperature crystallographic results (Table 4) are in accord with the phase diagrams (Stammler, 1968), which show that Rb and Cs picrates are completely mutually miscible, whereas K and Cs picrates have a large miscibility gap.

7.2. *Phase relations from DSC measurements*

DTA measurements were reported to show phase changes (endothermic on heating) in NH_4, K, Rb and Cs picrates at 483, 523, 516 and 553 K, respectively (Stammler, 1968); the structures of the high-temperature phases have not been reported. Our DSC measurements, using powdered samples, agree with those of Stammler. We have not investigated thermal events which appear to relate to high-temperature *chemical* reactions of the picrates. For NH_4 picrate, we find an endotherm at 476 K, with $\Delta H = 8.4$ kJ mol^{-1}. We have not investigated K picrate. For Rb picrate, we find an endotherm at 516 K, with $\Delta H = 9.1$ kJ mol^{-1}. For Cs picrate we find a complicated series of thermal events at *ca* 543 K, which we have not studied further. Stammler reports an endotherm at 553 K and an exotherm at *ca* 523 K on cooling, suggesting a reversible phase change with some hysteresis, and other thermal reactions at higher temperatures.

8. Summary

Thallium picrate is an example of a material with marked differences between the thermodynamic and kinetic behaviour of its two polymorphs. Although the thermodynamic equilibrium temperature is reported to be 319 K, transition from the red to the yellow polymorph occurs in the solid state at an appreciable rate only at 400 K and above. The yellow polymorph does not transform to red, neither on heating nor on cooling. The differences between the crystal structures of the two polymorphs are large enough to require the red-to-yellow transformation to be reconstructive, but we cannot explain why the transformation is not reversible on cooling. Addition of a small amount of solvent to the system remarkably accelerates the transformations (in both directions), but the details of these processes have still to be clarified. Reference is made to descriptions of the similar behaviour of other materials.

We are grateful to Professor A. Siegmann (Materials Engineering, Technion) for access to the Mettler Differential Scanning Calorimeter, and the Vice-President for Research and the Fund for the Promotion of Research at Technion for financial support. We acknowledge with thanks support for Dr Botoshansky from the Israel Ministry for Science and Technology.

References

AOKI, K., SUH, I.-H., NAGASHIMA, H., UZAWA, J. & YAMAZAKI, H. (1992). *J. Am. Chem. Soc.* **114**, 5722–5729.

BOTOSHANSKY, M., HERBSTEIN, F. H. & KAPON, M. (1994). *Acta Cryst.* B**50**, 191–200.

CHATTAWAY, F. D. & WÜNSCH, D. F. S. (1916). *J. Chem. Soc.* **119**, 2253–2265.

COHEN, E. (1929). *J. Soc. Chem. Ind.* **48**, 162–168.

COHEN, E. & MOESVELD, A. L. TH. (1920). *Z. Phys. Chem.* **94**, 450–464.

CROMER, D. T. (1974). *International Tables for X-ray Crystallography*, Vol. IV, Table 2.3.1, pp. 72–98. Birmingham: Kynoch Press. (Present distributor Kluwer Academic Publishers, Dordrecht.)

CROMER, D. T. & WABER, J. T. (1974). *International Tables for X-ray Crystallography*, Vol. IV, Table 2.2A, pp. 149–150. Birmingham: Kynoch Press. (Present distributor Kluwer Academic Publishers, Dordrecht.)

FINDLAY, A. (1951). *The Phase Rule and Its Applications*, 9th ed., edited by A. N. CAMPBELL & N. O SMITH. New York: Dover.

FISCHER, R. X. & TILLMANNS, E. (1988). *Acta Cryst.* C**44**, 775–776.

HARKEMA, S., BRAKE, J. H. M. TER & MEUTSTEGE, H. J. G. (1979). *Acta Cryst.* B**35**, 2087–2093.

HERBSTEIN, F. H., KAPON, M. & WIELINSKI, S. (1977). *Acta Cryst.* B**33**, 649–654.

JESSEN, S. M. & KÜPPERS, H. (1989). *Collected Abstracts of XIIth European Crystallographic Meeting*, Moscow, Vol. 1, p. 349 [published as Supplement No. 2 of *Z. Kristallogr.* (1990)].

JESSEN, S. M. & KÜPPERS, H. (1991). *J. Appl. Cryst.* **24**, 239–241.

JOHNSON, C. K. (1965). *ORTEP*. Report ORNL-3794. Oak Ridge National Laboratory, Tennessee, USA.

MAARTMAN-MOE, K. (1969). *Acta Cryst.* B**25**, 1452–1460.

MELLOR, J. W. (1956). *A Comprehensive Treatise on Inorganic and Theoretical Chemistry*, Vol. 2, p. 371. London: Longmans.

NYE, J. F. (1967). *Physical Properties of Crystals*, 1st ed. (corrected). Oxford: Clarendon Press.

OSAKE, S. (1949). *J. Chem. Soc. Jpn*, **70**, 96–98; *Chem. Abstr.* **45**, 4119h (1951).

PALENIK, G. J. (1972). *Acta Cryst.* B**28**, 1633–1635.

RABE, W. O. (1901). *Z. Phys. Chem.* **38**, 175–184.

SAX, N. I. (1979). Editor: *Dangerous Properties of Industrial Materials*. New York: Van Nostrand Reinhold.

SCHOMAKER, V. & MARSH, R. E. (1983). *Acta Cryst.* A**39**, 819–820.

SCHOUTEN, A., KANTERS, J. A. & POONIA, N. S. (1990). *Acta Cryst.* C**46**, 61–64.

SHANNON, R. D. (1976). *Acta Cryst.* A**32**, 751–767.

SHELDRICK, G. M. (1976). *SHELX76. Program for Crystal Structure Determination*. Univ. of Cambridge, England.

STAMMLER, M. (1968). *Explosivstoffe*, **16**, 154–163.

STEVANOVIC, S. (1903). *Z. Krist.* **38**, 257–266.

TAGUCHI, K., HIROTA, M., MAEDA, K., YASUI, M. & IWASAKI, F. (1993). Abstract PS-06.04.09 of XVIth Congress of International Union of Crystallography, Beijing, China.

TUINSTRA, F. & FRAASE STORM, G. M. (1978). *J. Appl. Cryst.* **11**, 257–259.